Photoactive TiO2–montmorillonite composite for degradation of organic dyes in water

Photoactive TiO_2-montmorillonite composite for degradation of organic dyes in water

R. Djellabi[a], M. F. Ghorab[a], G.Cerrato[c], S. Morandi[c], S. Gatto[b], V. Oldani[b], A. Di Michele[d], C.L. Bianchi[b*]

[a]*Laboratory of Water Treatment and Valorization of Industrial Wastes, Chemistry Department, Faculty of Sciences, Badji-Mokhtar University, BP12 2300, Annaba, Algeria*

[b]*Università degli Studi di Milano & Consorzio INSTM-UdR Milano, Dip.Chimica, Via Golgi, 19 – 20133 Milano, Italy*

[c]*Università degli Studi di Torino, Dipartimento di Chimica & NIS Interdept. Centre & Consorzio INSTM-UdR Torino, Via Giuria, 7 – 10125 Torino, Italy*

[d]*Università degli Studi di Perugia, Dipartimento di Fisica e Geologia, Via Pascoli – 06123 Perugia, Italy*

Corresponding author: claudia.bianchi@unimi.it

Abstract

TiO_2-montmorillonite composite (TiO_2-M) was prepared by impregnation with $TiCl_4$ followed by calcination at 350°C. The synthesized material was characterized by FTIR, TG-TDA, BET, XRD and SEM-EDX. The results show that TiO_2 was efficiently formed in Na-montmorillonite (Na-M) framework, and only a crystalline, pure anatase phase was produced. ~~The mean crystallite size is of about 15-20 nm~~. Photoactivity tests were carried out under UV-A irradiation using five selected organic dyes. The results ~~show~~ indicate that the activity of TiO_2-M is more important for cationic dyes, where the removal rates are in the order: Crystal violet (97.1%) > Methylene blue (93.20%) > Rhodamine B (79.8 %) > Methyl orange (36.1 %) > Congo red (22.6 %). The results of the TiO_2-M activity were compared with that of the commercial P25. The comparison demonstrates that the synthesized TiO_2-M exhibits a higher adsorptive behavior and can be used as low-cost alternative to the commercial TiO_2 for

wastewater treatment, showing also an extreme easiness to completely recover the composite catalyst at the end of the test.

Keywords: TiO_2-montmorillonite; Composite; Photoactivity; Dye; Decolourization; Water.

1. Introduction

Heterogeneous photocatalysis is becoming more interesting in recent years for several research areas, especially, for environmental applications [1, 2]. Among these applications, water remediation and in particular the decolourization of wastewaters is one of the most important area where scientific research has been focused [3, 4]. Among different kinds of photocatalysts, TiO_2 has been the most widely used for wastewater treatment because of its strong oxidizing properties for the removal of organic pollutants, super-hydrophilicity and chemical stability [1, 5]. It is known that the optical properties of TiO_2 and, as a consequence, its photoactivity, are strongly influenced by its characteristics like structure, morphology, particles size. For this purpose, many researchers have developed several methods for the preparation of new TiO_2 photocatalysts, with tailored features aimed at improving the final photoactivity towards the degradation of pollutants both in gas and water phase: TiO_2 nanopowders [6-8], N-doped carbon-TiO_2 [9, 10], doping of TiO_2 by transition metals [11] or noble metals [12] and TiO_2 in conjunction with other semiconductors [13-15].

Moreover, the photoactivity performances are strongly depended on the adsorption capacity of the photocatalyst, as it is known that the photocatalytic reaction occurs on the photocatalyst surface [16]. In order to improve the adsorption process, the immobilization of TiO_2 on porous materials like natural clays is a successful method. Furthermore, Ooka *et al.* reported that TiO_2/clay composites exhibit the advantage to photodecompose organic pollutants in water due to their hydrophobic interlayers [17]. TiO_2/clay composites have been synthesized by deposition (or pillaring) TiO_2 particles either on the surface of the clays or into their interlayers, thus obtaining dispersed TiO_2 nanoparticles with a high photoactivity. Different kinds of clays have been used. These included sepiolite [18], bentonite [19], kaolinite [20], zeolite [21] and montmorillonite [22]. Moreover, several methods have been used for the synthesis of TiO_2/clay composites. Such methods include the $TiCl_4$ adsorption followed by

calcination [23], sol-gel synthesis [24], $TiCl_4$ hydrolysis [25] and by wet grinding in an agate mill [26].

In the present work, a TiO_2-montmorillonite composite (TiO_2-M) was synthesized using a natural Na-montmorillonite impregnated with $TiCl_4$ and followed by calcination. Physico-chemical properties of the photocatalyst were determined by FTIR spectroscopy, TG-TDA, BET, XRD and SEM-EDX, whereas photoactivity was evaluated using five selected organic dyes in aqueous solution under UV-A irradiation. Photoactivity results were compared with those obtained employing the P25 by Evonik, a commercial sample often used as reference material in photocatalysis.

2. Materials and methods

2.1. Materials

The montmorillonite used in this study was a natural sodium-exchanged bentonite (Na-M) from the Roussel deposit in Maghnia (Algeria) and was used without any further treatment or purification. The cationic exchange capacity of Na-M, determined by methylene blue method [27], is 89.30 mmol/100 g.

TiO_2 P25 (Evonik) was used in the present study as a reference material. It is composed of approximately 80% anatase and 20% rutile, a BET surface area of 49 m^2/g and with crystallites size of about 25 nm [28].

Dyes used in this work were Cristal violet (Fluka), Rhodamine B (SIGMA-ALDRICH), Congo red (Fluka), Methylene blue (Fluka) and Methyl orange (SIGMA-ALDRICH). The structure of each dye is presented in Figure 1.

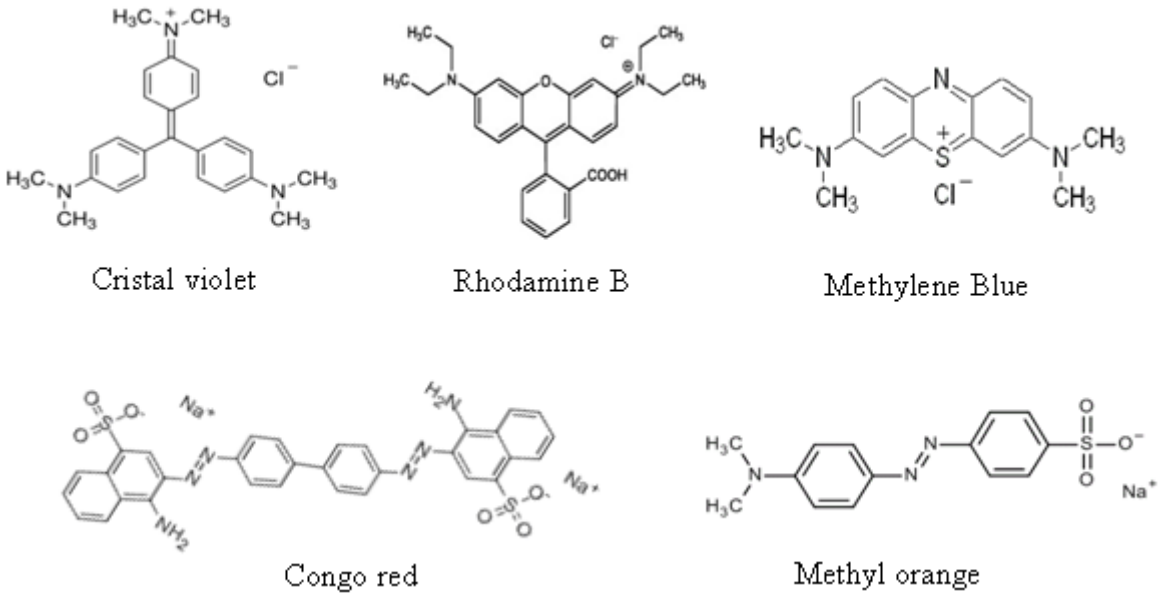

Figure 1. Chemical structure of different dyes used in this study

2.2. Synthesis of titania-montmorillonite

The photocatalyst synthesis method was similar to that reported by Rossetto *et al.*[29]. Titania-montmorillonite (TiO_2-M) was prepared by impregnation with $TiCl_4$ (Aldrich, 99.99%). Firstly, $TiCl_4$ was diluted with CH_2Cl_2 to obtain a clear solution. Then, the mixture was slowly added to Na-M suspension under vigorous stirring at 65°C for 4 hours under reflex system. The weight ratio of Ti/montmorillonite was 10% (g/g). The wet solid obtained was washed by double-distilled water, filtered and then dried at 110°C for 24 h: finally it was calcined in air at 350°C for 4 h.

2.3. Characterization

Fourier Transform InfraRed (FT-IR) spectra of Na-M and TiO_2-M (as self-supporting pellets, ~20 mg cm^{-2}) were recorded at room temperature at a 2 cm^{-1} resolution in the 4000-400 cm^{-1} spectral range using a Perkin–Elmer FT-IR System 2000 spectrophotometer, equipped with a

Hg–Cd–Te cryo-detector. The self-supporting pellets were posed in a quartz cell equipped with KBr windows: before recording the FTIR spectra, all samples have been activated in vacuo connecting the cell to a vacuum line (residual pressure < 10^{-4} mbar). Thermogravimetry-Differential Thermal Analysis (TG-DTA) was performed using a thermo-gravimetric analyzer (NETZSCH STA 409 PC/PG) at a heat rate of 10 °C/min from 25 to 500°C under air atmosphere.

The BET specific surface areas were determined using a Thermo Quest Sorptomatic 1990 Technical Specification instrument.

The morphology of Na-M and TiO_2-M particles was determined by Field Emission Scanning Electron Microscopy (FEG LEO 1525, ZEISS Company, Germany). The Energy Dispersion X-ray Spectroscopy (EDS) analysis (Quantax 200 with Xflash 400 detector,Bruker Company, Germany), coupled with the Scanning Electron Microscopy, was used to analyze the elements content of the samples.

The XRD patterns were recorded on a diffractometer instrument (Philips PW3830/3020 X'Pert diffractometer, PANalytical) using monochromatized CuKα radiation at 1= 1.54 Å. The interlayer d-spacing reflection was calculated using the Bragg equation [30]. The crystallite size of anatase TiO_2 was calculated using Scherrer's formula.

3.4. Photocatalytic tests

The photocatalytic experiments were carried out in a static quartz reactor (500 mL), equipped with a cold finger to avoid thermal reactions (Figure 2). A UV-A lamp (λmax = 365nm, 100W/m^2) was placed next to the reactor at 10 cm. In a typical experiment, 0.08 g of the photocatalyst and 500 mL of dye solution at 10^{-4} mol/L were stirred under irradiation for 6 h. During the reaction, samples were collected at selected time intervals. The adsorption experiments were performed under the same conditions without irradiation. The powdered

photocatalysts were removed by filtration (0.45 µm, Whatman) and the residual concentration of dyes was determined using a UV–visible spectrophotometer (T60 PG Instruments).

The removal rate of the dyes was calculated using the following equation:

$$R(\%) = \frac{(C_0 - C_t)}{C_0} \times 100 \qquad (1)$$

Where C_0 and C_t represent the dye concentration (mol/L) before and after reaction.

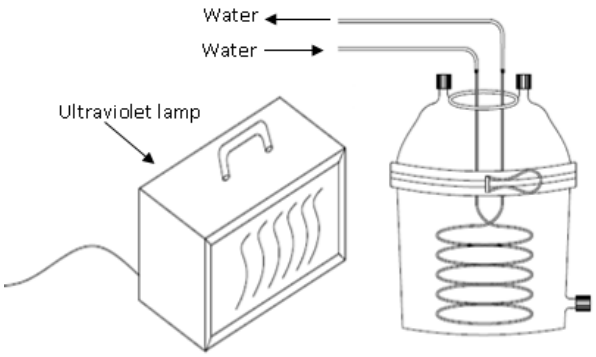

Figure 2. Scheme of the photoreactor

3. Results and discussion

3.1. Physico-chemical characterization

3.1.1. FTIR

Figure 3 shows the FTIR spectra (in the 4000-1200 cm^{-1} range) of Na-M and TiO_2-M obtained after activation *in vacuo* at room temperature (RT).

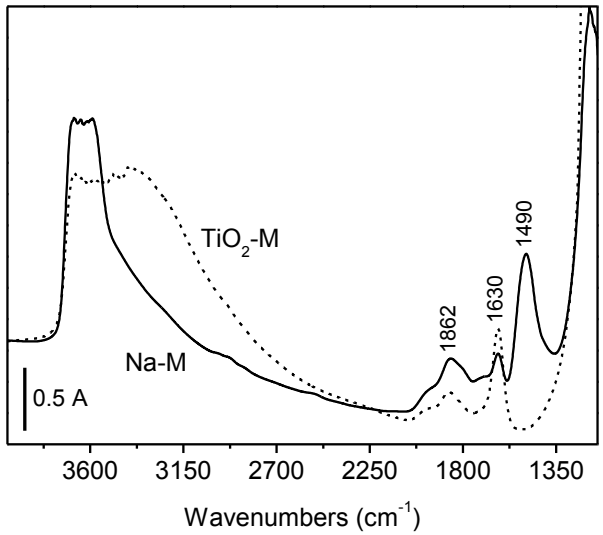

Figure 3.FTIR spectra of Na-Mand TiO_2-Mafter activation in vacuo at RT.

For both samples there are present bands in the 3700-3000 cm^{-1} range: on the basis of their spectral behavior and of literature data [31-33], they can be assigned to the stretching vibration modes of all (either structural and/or surface) OH groups mutually interacting by H-bonding. The spectroscopic counter part of these modes can be observed at ~1630 cm^{-1}: it corresponds to the bending mode of all undissociated H_2O molecules present in/on the materials. Moreover, in the 2000-1700 cm^{-1} range a complex envelope of bands is present for both materials: it can be assigned to the typical overtones of the SiO_2-like matrix [34]. On the other hand, it is worth noting that Na-M exhibits a sharp and complex spectral component at ~ 1490 cm^{-1}: this component, totally absent in the case of TiO_2-M, is ascribable to some modes typical of carbonate anions [35]. The absence of this component in the TiO_2-containing material can be related to the addition of TiO_2, as reasonably in the synthetic step the anions present in the interlayers of the montmorillonite material are totally substituted by the anions formed by titanium-containing species. In the calcination step, the presence of the latter

species brings about the formation of TiO_2 and leads to the retaining of a higher amount of water, as evidenced in TiO_2-M spectrum reported in Figure 3: the envelope assigned to the OH stretching mode and the component located at 1630 cm^{-1} (bending mode of undissociated molecular water) are much larger/more intense in the case of TiO_2-M.

3.1.2. TG/DTA

The TG/DTA curves of Na-M and TiO_2-M samples in the temperature range from 25 to 500 °C are reported in Figure 4. The TG curve shows weight loss in two stages of 25-200 and 200-500°C for both samples. The first stage corresponds to a weight loss of 11.18 and 5.66 % for Na-M and TiO_2-M, respectively. This mass change is due to the evaporation of physisorbed water [24, 36]. The DTA curve exhibits endothermic peaks at 99.5 °C (Na-M) and 105.4 °C (TiO_2-M) which confirms the loss of adsorbed water. The lower mass change in the case of TiO_2-M, if compared to Na-M, can be related to the presence of TiO_2 itself, and also confirmed by the major amount of OH groups observed in the FTIR spectra after activation *in vacuo* (see Figure 3). The second stage shows a lower weight loss of 0.50% and 1.03% for Na-M and TiO_2-M, respectively. This is due to desorption of more strongly adsorbed water [37].

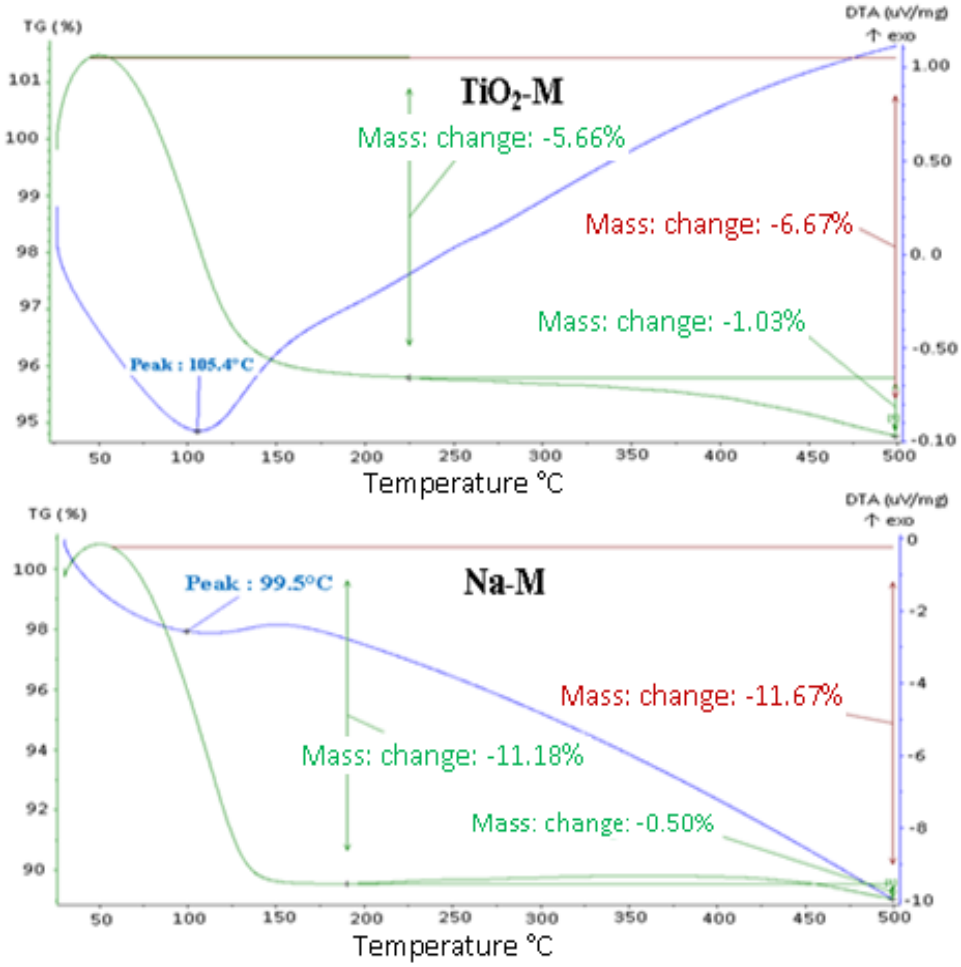

Figure 4.TG/DTA of Na-M and TiO_2-M samples

3.1.3. Specific surface area and porosity measurements

The BET specific surface area of the Na-M and TiO_2-M samples is shown in Table 1. It can be seen that the introduction of TiO_2 changes to a very limited extent the value of surface area of the starting material (49.4 to 51.5 m^2/g). The change of the pore volume is more evident (from 0.107 to 0.144 cm^3/g): it might be related to the addition of TiO_2. As a matter of fact, for both samples the isotherms related to adsorption/desorption branch of N_2 at 77K exhibit the shape typical of mesoporous materials and belong to type 2, with an evident hysteresis loop of type H_3 [38]. Moreover, if we analyse these data applying the BJH method, we can

preliminary conclude that both materials exhibit a net mesoporosity with a medium pore width of ~ 40 Å.

Table 1 Result of adsorption–desorption measurements

Samples	Specific surface area (m^2/g)	Pore volume (cm^3/g)
Na-M	49.4	0.107
TiO_2-M	51.5	0.144

3.1.4. XRD

The XRD patterns of Na-M and TiO_2-M samples are reported in Figure 5. The small angle XRD pattern of Na-M shows a strong peak at 2Θ=5.87° due to the d(100) basal spacing reflection of the montmorillonite [39]. In the case of the TiO_2-M sample this peak is split into two components located at 2Θ = 5.68° and 7.47°: this splitting is a clear indication that the introduction of TiO_2 brings about a decreasing of the basal spacing of a part of the montmornillonitic material. The latter result demonstrates that the titanium species are really inserted in the montmonillonite interlayers. On the wide-angle diffraction, in the TiO_2-M diffractogram we observe the typical peaks ascribable to a montmonillonite material; moreover, titanium crystallization reflections are also observed, in which only the anatase polymorph is evidenced. The average crystallite size of anatase was estimated of ~ 15-20 nm employing the (101) reflex for the calculation.

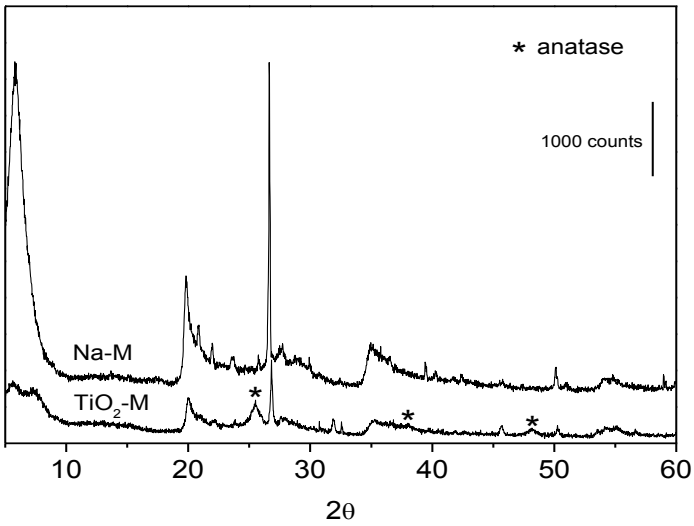

Figure 5. XRD patterns of Na-M and TiO_2-M samples.

3.1.5. SEM-EDX

Figure 6 reports the SEM images of Na-M and TiO_2-M. The Na-M sample has a spongy integrated flakes-like structure; furthermore, it exhibits some smooth regions in its structure. The TiO_2-M image shows a clear change of the montmorillonite morphology: this feature can be ascribed to the decreasing of the interlayer spacing brought about by the addition of TiO_2, as also indicated by the XRD characterization.

The results of the EDS analysis of Na-M and TiO_2-M are reported as numerical values in Table 2. The results of the elemental analysis of Na-M indicate that Si and Al are the main constituents of the material, which are estimated to be 60.06 and 20.81 wt%, respectively. Furthermore, Na content in Na-M is larger than that of Ca. The content of Ti element in TiO_2-M is 48.6 wt%. The high Ti content observed is much more than that added from $TiCl_4$ during the preparation (which was only 10 wt %). This is related to the calcination step operated at 350°C: as revealed by TG/DTA measurements, the loss of both adsorbed and structural water justifies the observed increasing of the Ti content [22].

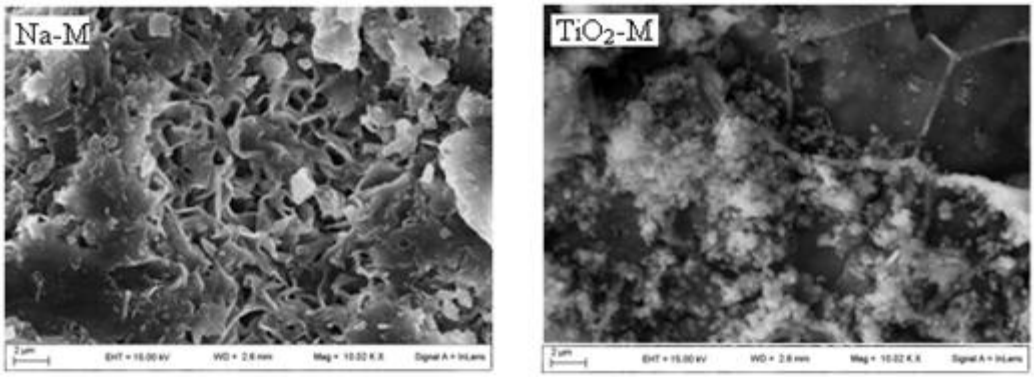

Figure 6. SEM images of Na-M (left-hand section) and TiO_2-M (right-hand section) samples.

Table 2 Elemental analysis of Na-M and TiO_2-M

Element [w%]	**Si**	**K**	**Al**	**Mg**	**Fe**	**Na**	**Ca**	**Cl**	**Ti**
Na-M	60.06	1.03	20.81	5.37	6.07	4.84	1.25	0.57	-
TiO_2-M	25.26	1.27	8.58	1.64	2.24	3.25	1.48	7.72	48.56

3.2. Photocatalytic activity

The results of the decolourization of different dyes using both P25 and TiO_2-M under UV-A irradiation compared with direct photolysis and dark adsorption are reported in Figures 7-11. Furthermore, the removal rates of different dyes are summarized in Table 3. From these results it can be observed that, after 6 h, the direct photolysis was different for each dye and was in the order: Methylene blue (20.6 %) > Rhodamine B (10.3 %) > Congo red (6.2 %) > Crystal violet (5.7 %) > Methyl orange (4.4 %).

The results of the dark adsorption on the P25 were in the range of 6.0 % to 18.6 %, where the Congo red and the Crystal violet possess the highest values. The photodegradation rates of dyes by P25 were higher than 80% except for the Methyl orange (59.6 %). In the case of

TiO_2-M, the dark adsorption effectiveness of the same dyes follows the order: Methylene blue (67.6 %) > Crystal violet (58.8 %) > Rhodamine B (45.0 %) > Methyl orange (14.9 %) > Congo red (6.2 %), reflecting the higher adsorptive capacity of the cationic dyes (Methylene blue, Crystal violet and Rhodamine B). On the other hand, the anionic dyes show a smaller adsorption. This is due to less attraction charges of TiO_2-M for the anionic dyes. The dissimilarity observed between P25 and TiO_2-M on the adsorption rate of dyes can be explained by the different proprieties and morphologies of these materials. The surface of TiO_2-M is porous and spongy, on the contrary TiO_2 P25 particles exhibit a smooth surface. Furthermore, the high cation exchange capacity of TiO_2-M due to negative charge in its interlayer increases the attraction and the adsorption of cationic dyes [40]. In addition, the point of zero charge (PZC) of TiO_2 P25 is reported to be in the pH range of 6-7.5 [41], which is near to our pH range working. At this point, the surface charge is null thus resulting to be less attractive to the dye molecules.

The photodegradation of dyes by TiO_2-M is in the order: Crystal violet (97.1 %) > Methylene blue (93.2 %)>Rhodamine B (79.8 %) > Methyl orange (36.1 %) > Congo red (22.6 %). It is worth mentioning the similarity in the orders obtained in the adsorption and photodegradation of the dyes under investigation. These results confirm the relationship between the adsorption and the photocatalytic activity, as the photodegradation reaction of organic pollutants occurs after their adsorption on the surface [40]. It is important to note that the adsorption behavior of this material contributes simultaneously to accelerate the photocatalytic action and to participate for the total removal of dyes. Hence, the total degradation rate of dyes should include an adsorption part of dye especially when dye molecules are accumulated inside the pores of TiO_2-M: in this case, UV irradiation and produced radicals cannot reach them. Furthermore, it is difficult to evaluate the adsorption contribution in the degradation rate, but

we can ensure that this material combines the adsorption and the photocatalytic reaction to remove dyes from water.

The comparison between P25 and the synthesized TiO_2-M composite demonstrates the advantages of this latter with a high adsorptive behavior and a cation exchange capacity of 96.5 mmol/100g, which favours the adsorption of a larger number of dye molecules. Consequently, it facilities their degradation by the photoactive deposed TiO_2 particles, leading to a higher concentration of dye molecules around the TiO_2 particles as compared to that in the bulk solution, resulting in an increase in the degradation rate [42-43]. In addition, the adsorptive behavior of TiO_2-M may contribute to the fixation of the intermediates produced during the degradation in order to be further oxidized.

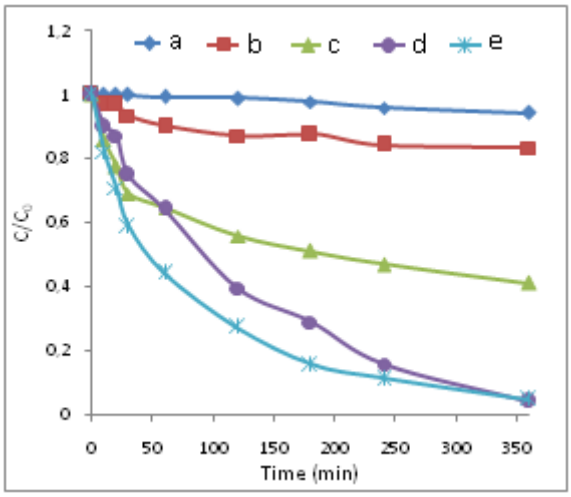

Figure 7. Photocatalytic decolorization of Crystal violet. (a):photolysis, (b):P25 (dark), (c): TiO_2-M (dark), (d): P25 (UV), (e): TiO_2-M (UV).

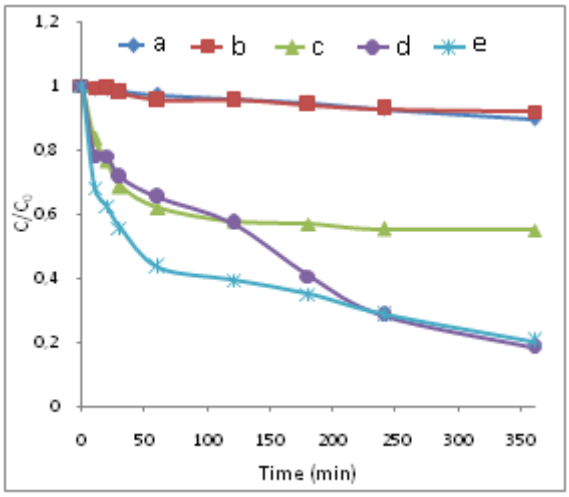

Figure 8. Photocatalytic decolorization of Rhodamine B. (a): photolysis, (b):P25 (dark), (c): TiO_2-M (dark), (d): P25 (UV), (e): TiO_2-M (UV).

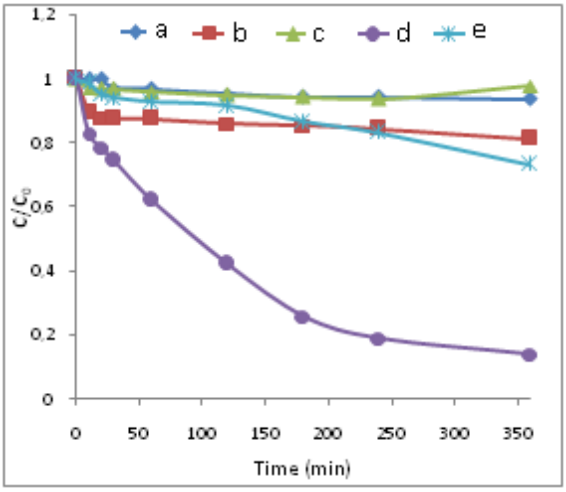

Figure 9. Photocatalytic decolorization of Congo red. (a): photolysis, (b):P25 (dark), (c): TiO_2-M (dark), (d): P25 (UV), (e): TiO_2-M (UV).

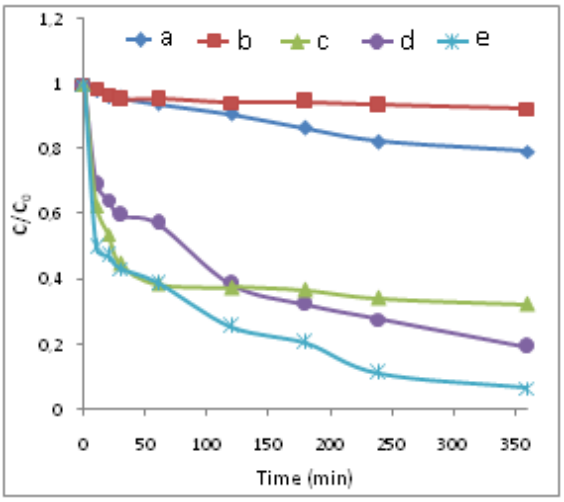

Figure 10. Photocatalytic decolorization of Methylene blue. (a):photolysis, (b): P25 (dark), (c): TiO_2-M (dark), (d): P25 (UV), (e): TiO_2-M (UV).

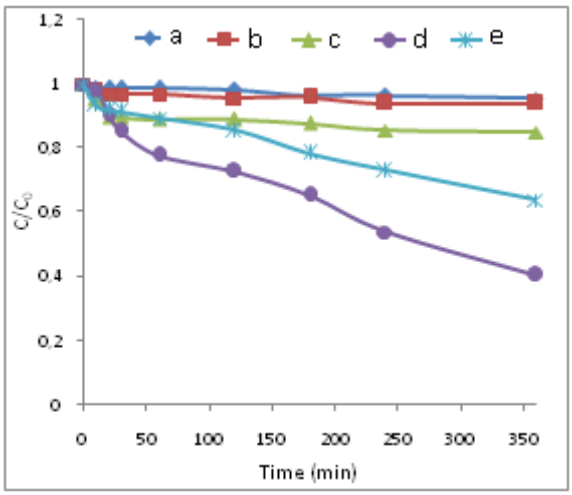

Figure 11. Photocatalytic decolorization of Methyl Orange. (a):photolysis, (b):P25 (dark), (c): TiO_2-M (dark), (d): P25 (UV), (e): TiO_2-M (UV).

Table 3. Comparison of the removal rates of different dyes using P25 and TiO_2-M

		Removal rate (%)				
		Crystal violet	Congo red	Methylene blue	Methyl orange	Rhodamine B
	Photolysis	5.7	6.2	20.6	4.4	10.3
P25	In dark	16.5	18.6	7.6	6.0	8.1
	Under UV	95.8	85.9	80.7	59.6	81.2
TiO_2-M	In dark	58.8	6.2	67.6	14.9	45.0
	Under UV	97.1	22.6	93.2	36.1	79.8

4. Conclusions

TiO_2-montmorillonite was synthesized using a simple method which consists in the impregnation of the clay with $TiCl_4$ followed by calcination.

The characterization results show that TiO_2 particles were, at least in part, introduced in the interlayer spaces. of the montmorillonite. The Ti content in TiO_2-M was 48.6 wt% with an anatase crystallite size of about 15-20 nm. The adsorption effectiveness and the photocatalytic degradation reactions of TiO_2-M were more pronounced for the cationic dyes. Additionally, the photoactivity of TiO_2-M increases when the dye molecules are more adsorbed: this is due to the increase of the contact between the TiO_2 particles deposed on the TiO_2-M surface and the dye molecules.

The use of TiO_2-M composite for water treatment is an attractive alternative to the commercial TiO_2 taking into account the higher adsorptive behavior, its low-cost and also its rapid recovery at the end of the test by simple filtration.

References

[1] K.Nakata, A. Fujishima, TiO_2 photocatalysis: Design and applications, J.Photochem.Photobiol. C. 13 (2012) 169–189.

[2] M.R., Hoffmann, S.T. Martin, W.Choi, D.W.Bahnemann, Environmental applications of semiconductor photocatalysis, Chem. Rev. 95(1) (1995) 69-96.

[3]J-M.Herrmann, Heterogeneous photocatalysis: fundamentals and applications to the removal of various types of aqueous pollutants, Catal. Today 53 (1999) 115–129.

[4] K. Kavita, C.Rubina, L.S. Rameshwar, Treatment of hazardous organic and inorganic compounds through aqueous-phase photocatalysis: a review, Industrial Eng in. Chem. Res. 43(2004) 7383–7696.

[5] V.A. Sakkas,I.M.Arabatzis,I.K.Konstantinou, A.D.DimouAlbanis,P. Falaras, Metolachlor photocatalytic degradation using TiO_2 photocatalysts, App.Catal. B: Environ.49 (2004) 195–20.

[6] A.Hosseinnia, M.Keyanpour-Rad,M.Kazemzad, M.Pazouki, A novel approach for preparation of highly crystalline anatase TiO_2nanopowders from the agglomerates, Powder Technol.190 (2009) 390–392.

[7] M. Caplovicová, P. Billik, L. ˇCaplovic, V. Brezová, T. Turáni, G. Plesch, P.Fejdi, On the true morphology of highly photoactive anatase TiO_2nanocrystals. App. Catal.B: Environ. 117-118(2012) 224–235.

[8] S.Ardizzone, C.L. Bianchi, G.Cappelletti, S. Gialanella, C. Pirola, V. Ragaini, Tailored anatase/brookitenanocrystalline TiO_2. The optimal particle features for liquid- and gas-phase photocatalytic reactions,J. Phys.Chem.C 111 (2007) 13222-13231.

[9] H. Ming,H. Huang, K. Pan, H. Li, Y. Liu,Z. Kang, C/TiO_2nanohybrids co-doped by N and their enhanced photocatalytic ability, J. Solid State Chem. 192 (2012) 305–311.

[10] S V. Trevisan, A. Olivo, F. Pinna, M. Signoretto, F. Vindigni, G. Cerrato, C.L. Bianchi, Investigation on the Stability of Supported Gold Nanoparticles, App. Catal. B, in press.

[11] M.I. Litter, Heterogeneous photocatalysis: Transition metal ions in photocatalytic systems, App. Catal. B: Environ. 23 (1999)89-114.

[12] M. Ni, M.K.H. Leung, D.Y.C. Leung, K. Sumathy, A review and recent developments in photocatalytic water-splitting using TiO_2 for hydrogen production, Sustain. En.Rev. 11 (2007) 401-425.

[13] D.L. Liao, C.A. Badour, B.Q. Liao, Preparation of nanosized TiO_2/ZnO composite catalyst and its photocatalytic activity for degradation of methyl orange, J.Photochem.Photobiol. 194(2008) 11–19.

[14] S. Bai, H. Li, Y. Guan, S. Jiang, The enhanced photocatalytic activity of CdS/TiO_2nanocomposites by controlling CdS dispersion on TiO_2 nanotubes, App. Surf. Sci. 257(2011) 6406–6409.

[15] B. Neppolian, A. Bruno, C.L. Bianchi, M. Ashokkumar, Graphene oxide based Pt–TiO_2 photocatalyst: Ultrasound assisted synthesis, characterization and catalytic efficiency, Ultras. Sonochem. 19 (2012) 9-15.

[16] D.S. Bhatkhande, V.G. Pangarkar, A.A.C.M. Beenackers, Photocatalytic degradation using TiO_2 for environmental applications – A review, J. Chem. Technol. Biotechnol. 77 (2002) 102–116.

[17] C. Ooka, H. Yoshida, M. Horio, K. Suzuki, T. Hattori, Adsorptive and photocatalytic performance of TiO_2 pillared montmorillonite in degradation of endocrine disruptors having different hydrophobicity, App. Catal. B: Environ. 41 (2003) 313–321.

[18] Z.M. Xie Chen,Y. Z. Dai, Preparation of TiO_2/sepiolite photocatalyst and its application to printing and dyeing wastewater treatment, Environ. Sci. Technol. 32(2009) 123-127.

[19] Z. Sun,Y. Chen, Q. Ke, Y. Yang, J. Yuan, Photocatalytic degradation of a cationic azo dye by TiO_2/bentonite nanocomposite, J. Photochem. Photobiol. A: Chem. 149(2002)169-174.

[20] M. N. Chong, V. Vimonses, S. Lei, B. Jin, C. Chow, C. Saint, Synthesis and characterization of novel titania impregnated kaolinite nano-photocatalyst, Micropor. Mesopor. Mater. 117(2009) 233-242.

[21] M. Mahalakshmi, S. Vishnu Priya, B. Arabindoo, M. Palanichamy, V. Murugesan, Photocatalytic degradation of aqueous propoxur solution using TiO_2 and H_β zeolite-supported TiO_2, J. Haz. Mater. 161 (2009) 336–343.

[22] Y. Kameshima, Y. Tamura, A. Nakajima, K. Okada, Preparation and properties of TiO_2/montmorillonite composites, App. Clay Sci. 45 (2009) 20-23.

[23] G. Grubert, M. Wark, N. I. Jaeger, G. Schulz-Ekloff, O. P.Tkachenko, Reduction kinetics of zeolite-hosted mono- and polynuclear titanium oxide species followed by UV/Vis diffuse reflectance spectroscopy: influence of location and coordination, J. Phys. Chem. B 102 (1998) 1665–1671.

[24] L. Xiang, X. Zhao, Preparation of montmorillonite/titania nano-composite and enhanced electro-rheological activity, J. Colloid. Inter. Sci. 296 (2006) 131–140.

[25] J. Liu, X. Li, S. Zuo, Y. Yu, Preparation and photocatalytic activity of silver and TiO_2nanoparticles/montmorillonite composite, App. Clay Sci. 37(2007) 275–280.

[26] M. Judit, K. László, E. Bazsó, Z. Volker, R. André, D. Imre, Photocatalytic oxidation of organic pollutants on titania–clay composites, Chemosphere 70 (2008) 538–542.

[27] P.T. Hang, G. W. Brindley, Methylene blue absorption by clay minerals. Determination of surface areas and cation exchange capacities (clay-organic studies XVIII), Clays and Clay Miner. 18 (1970) 203-212.

[28] G. Cerrato, L. Marchese, C. Morterra, Structural and morphological modifications of sintering microcrystalline TiO_2: an XRD, HRTEM and FTIR Study, Appl. Surf. Sci. 70/71 (1993) pp. 200-205

[29] E. Rossetto, D.I. Petkowicz, J. H. Z. dos Santos, S. B. C. Pergher, F. G. Penha, Bentonites impregnated with TiO_2 for photodegradation of methylene blue, Appl. Clay Sci. 48 (2010) 602–606.

[30] Y. Li, J. R. Liu, S. Y. Jia, J. W. Guo, J. Zhuo, P. Na, TiO_2 pillared montmorillonite as a photoactive adsorbent of arsenic under UV irradiation,Chem. Eng. J. 191 (2012) 66–74.

[31] L.H. Little, Infrared Spectra of Adsorbed Species, Academic Press. London (1966).

[32] C. Morterra, An infrared spectroscopic study of anatase properties. Part 6.—Surface hydration and strong Lewis acidity of pure and sulphate-doped preparations, J. Chem. Soc. 84 (1988) 1617–1637.

[33] C. Morterra, V. Bolis, E. Fisicaro, The hydrated layer and the adsorption of CO at the surface of TiO_2 (anatase), Colloids Surf. 41 (1989) 177–188.

[34] A. P. Legrand, The Surface Properties of Silicas, John Wiley and Sons. New York (1998).

[35] G. Busca, V. Lorenzelli, Infrared spectroscopic identification of species arising from reactive adsorption of carbon oxides on metaloxide surfaces, Mater. Chem. 7 (1982) 89–126.

[36] B. Z. Lin, X. L. Li, B. H. Xu, Y. L. Chen, B. F. Gao, X. R. Fan, Improved photocatalytic activity of anatase TiO_2-pillared $HTaWO_6$ for degradation of methylene blue, Micropor. Mesopor. Mater. 155 (2012) 16–23.

[37] B. Dou, H. Chen, Y. Song, C. Tan, Synthesis and characterization of hetero-structured nanohybrid of MgO-TiO_2-Al_2O_3/montmorillonite, Mater. Chem. Phys. 130 (2011) 63– 66.

[38] S.J. Gregg, K. S. W. Sing, Adsorption, Surface Area and Porosity, Academic Press London. (1992).

[39] I. Fatimah, S. Wang, K. Wijaya, Composites of TiO_2-aluminum pillared montmorillonite: synthesis, characterization and photocatalytic degradation of methylene blue, App. Clay Sci. 50 (2010) 588–593.

[40] G. Kahr, F.T. Madsen, Determination of the cation exchange capacity and the surface area of bentonite, illite and kaolinite by methylene blue adsorption, Appl. Clay. Sci., 9 (1995) 327-336.

[41] A. Fernandez-Nieves, C. Richter, F.J. de las Nieves, Point of zero charge estimation for a TiO_2/water interface, Prog. Colloid Sci., 110 (1998) 21-24.

[42] J. Liu, M. Dong, S. Zuo, Y. Yu, Solvothermal preparation of TiO_2/montmorillonite and photocatalytic activity, App. Clay Sci. 43 (2009) 156–159.

[43] J. Matos, A. Garcia, T. Cordero, J.-M. Chovelon, C. Ferronato, Eco-friendly TiO_2-AC photocatalyst for the selective photooxidation of 4-Chlorophenol, Catal. Lett. 130 (2009) 568-574.